Chapter 24
Molecularly Targeted Staging Strategies in Renal Cell Carcinoma

Steven G. Koopman, Ali-Reza Sharif-Afshar, Robert A. Figlin, and Hyung L. Kim

Introduction

In the United States, it is estimated that in 2013, approximately 65,150 new cases of renal malignancies will be diagnosed and more than 13,680 individuals will die of the disease [1]. As many as 30 % of patients have metastatic disease at the time of initial diagnosis, and approximately 30 % of patients diagnosed with organ-confined disease develop recurrence following nephrectomy [2, 3]. The prognosis associated with renal cell carcinoma (RCC) can vary widely. Metastatic or recurrent RCC carries a poor prognosis and long-term survival is rare. Historically, the 3-year survival rate for patients with metastatic disease is less than 5 % [4]. However, many small RCCs that are incidentally discovered have an indolent course even without treatment. Thus, accurate diagnosis, staging, and determination of prognosis are useful for patient counseling, selecting treatment, and considering enrollment for clinical trials.

Ideally, diagnosing and staging of any malignancy is performed without invasive procedures and with minimal risk of morbidity. Cancer staging involves determining the extent cancer has progressed by spreading. In routine clinical practice, cancer is staged using imaging studies such as x-ray, high-resolution computerized tomography (CT) scans, and magnetic resonance imaging (MRI). However, the resolution of current imaging studies limits the accuracy of staging. Therefore, an important goal of modern imaging research is to assess tumor tissue at the molecular

S.G. Koopman, M.D. • A.-R. Sharif-Afshar, M.D. (✉) • H.L. Kim, M.D.
Department of Surgery/Urology, Cedars-Sinai Medical Center,
8635 West Third Street, Suite 1070W, Los Angeles, CA 90048, USA
e-mail: koopmanS@cshs.org; Ali.Afshar@cshs.org; kimhL@cshs.org

R.A. Figlin, M.D., F.C.A.P.
Department of Hematology/Oncology, Cedars-Sinai Medical Center,
8700 Beverly Blvd, 1S28 Saperstein Critical Care Tower, Los Angeles, CA 90048, USA
e-mail: Robert.Figlin@cshs.org

R.M. Bukowski et al. (eds.), *Renal Cell Carcinoma*,
DOI 10.1007/978-1-4939-1622-1_24

level to improve staging accuracy. The term molecular imaging refers to a wide variety of imaging strategies designed to visualize tumors at the cellular level or provide information about cellular function, including proliferative state and metabolic state. In the era of targeted therapies, molecular imaging has the potential to identify molecular signatures to help direct treatment and monitor response, without need for invasive biopsies. In this chapter, we review current molecular imaging techniques that have been proposed for RCC.

Molecular Imaging Techniques

Imaging modalities can be classified by the information they provide. Imaging can provide information about anatomy, physiology, cellular function, or molecular state. Standard imaging (e.g., CT, MRI, and ultrasound) provides information on anatomy and physiology. Molecular imaging provides information on cellular function or molecular state. We will concentrate on the molecular imaging strategies currently being used in RCC staging, which can be broadly categorized as positron emission tomography (PET) and optical imaging.

PET Imaging

PET is a nuclear medicine imaging technique which produces images that reflect functional processes. To produce these images, a biologically active molecule is tagged with a positron-emitting radionuclide (tracer) and introduced into the body. The active molecule is taken up by the target tissue and concentrated. After imaging the tissue for gamma rays and obtaining a CT scan, computer analysis is performed to obtain three-dimensional images that localize the tracer in the body. PET tracers are commonly produced using isotopes of elements often occurring in natural biological compounds such as fluorine and iodine. The characteristic molecular defect in clear cell RCC (ccRCC) is the inactivation of the von Hippel-Lindau (pVHL) protein. This defect contributes to upregulation of hypoxia-inducible factor (HIF) and subsequent transcription of hypoxia-regulated genes, including angiogenic factors such as vascular endothelial growth factor (VEGF), platelet-derived growth factor (PDGF), glucose transporter (Glut), and carbonic anhydrase IX (CAIX). Several drugs that target angiogenesis have recently been approved for RCC. One of the first targeted therapies approved for RCC is sunitinib, which inhibits the receptors for VEGF and PDGF. Since the uptake of certain PET radiotracers (e.g., ^{18}F-fluorodeoxyglucose and ^{124}I-girentuximab) is dependent on HIF signaling, PET has a potential role in RCC imaging and may even report the modulation of the HIF pathway by targeted drugs such as sunitinib [5–7]. In the following sections, we review currently available PET radiotracers being used for RCC (Table 24.1).

Table 24.1 Diagnostic PET imaging for RCC

Imaging type	Study	Tumor site	Year	*n*	Sensitivity	Specificity
FDG-PET	Wang et al. [10]	Renal	2012	Meta-analysis (14 studies)	62 %	88 %
		Extrarenal			79 %	90 %
		Extrarenal[a]			91 %	88 %
FDG-PET	Kang et al. [8]	Renal	2004	66	60 %	100 %
		Extrarenal	2004		75 %	100 %
FDG-PET	Nakatani et al. [9]	Recurrence	2009	23	81 %	71 %
FDG-PET/CT	Kayani et al. [11]	Renal/ extrarenal[b]	2011	44	87 %	95 %
^{124}I-cG250-PET/CT	REDECT trial [17]	Renal	2013	195	86.2 %	85.9 %
^{111}In-Bevacizumab PET	Desar et al. [22]	Renal	2010	14	Accumulated in all patients with RCC	

[a]FDG-PET/CT
[b]PET-predicted response to sunitinib

^{18}F-Fluorodeoxyglucose (FDG) PET

FDG is an analog of glucose, and FDG uptake indicates glucose uptake and metabolic activity. The sensitivity and specificity of FDG-PET are somewhat limited for primary tumors because the normal kidney has high background uptake of the radiotracer (Figs. 24.1 and 24.2). However, FDG-PET may be more useful for imaging metastatic lesions (Fig. 24.3). Kang et al. [8] reported their experience with FDG-PET in 66 patients with either primary, metastatic RCC or local recurrence of RCC. Rapid progression to death due to RCC, growth on follow-up imaging, or histopathologic confirmation served as the "gold standard" for assessing the imaging results. The results of PET were compared with conventional imaging. In primary RCC, PET was 60 % sensitive and 100 % specific. For nodal metastases in the retroperitoneum and/or local recurrence, PET was 75 % sensitive and 100 % specific. PET had a sensitivity of 77 and 100 % specificity for bone metastases. However, 6 out of 52 patients had metastatic disease detected on conventional imaging that was missed on PET.

In a study by Nakatani et al. [9], 23 postsurgical patients were evaluated for recurrent disease using FDG-PET. Diagnostic accuracy was evaluated by comparison with the final diagnosis determined histologically or by growth on follow-up imaging. The recurrent disease was seen in 21 of 28 cases. The sensitivity of PET imaging for detecting recurrent disease was 81 % and the specificity was 71 %. It was noted that PET detected all intra-abdominal and bone recurrences.

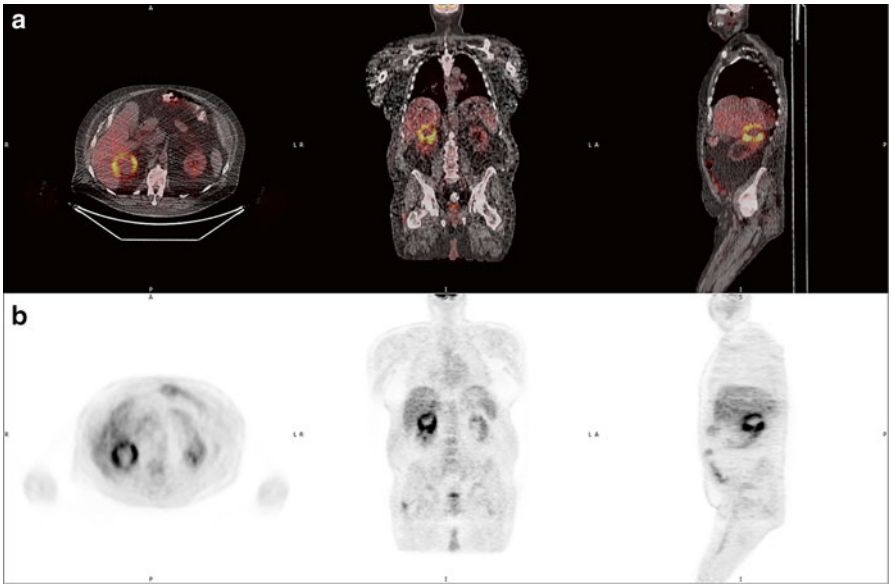

Fig. 24.1 ^{18}F-Fluorodeoxyglucose (FDG) PET/CT scan of a clear cell renal tumor located on the right kidney (**a**), FDG-PET scan that was fused to the CT scan (**b**). The tumor is metabolically active at the periphery and has a necrotic center

Wang et al. [10] performed a meta-analysis of 14 eligible studies. The sensitivity and specificity of FDG-PET for detection of primary RCC lesions were 62 % and 88 %, respectively. However, both sensitivity and specificity were higher for detecting extrarenal lesions, 79 % and 90 %, respectively, and they were further increased to 91 % and 88 %, respectively, with the use of hybrid FDG-PET/CT.

FDG-PET/CT was evaluated by Kayani et al. [11] as an imaging tool to assess the response to sunitinib in 44 patients with metastatic RCC. In a phase II prospective multicenter trial of sunitinib, patients were evaluated with FDG-PET/CT prior to treatment and after 4 and 16 weeks of treatment. FDG-PET/CT had a sensitivity of 87 % and specificity of 95 % for detecting tumor site pretreatment, suggesting a potential role for FDG-PET/CT in initial staging. For each patient, the lesion with the most intense standard uptake value (SUV) was used as the index lesion. Metabolic response was defined as a decrease in SUV by >20 %, and disease progression was defined as an increase in SUV by ≥20 % or development of a new metastatic site. After 4 weeks of treatment, 24 (57 %) patients had a metabolic response, but this did not correlate with progression-free survival (PFS) or overall survival (OS). After 16 weeks of treatment, 12 (24 %) patients had metabolic progression after 16 weeks of treatment. This progression correlated with a decreased OS and PFS. Patients with FDG-PET/CT progression at 16 weeks had more metabolically active disease at baseline and the majority had an initial metabolic response to sunitinib (10 of 12 patients). The traditional radiological methods of monitoring disease response to systemic treatment, such as response evaluation criteria in solid tumor (RECIST),

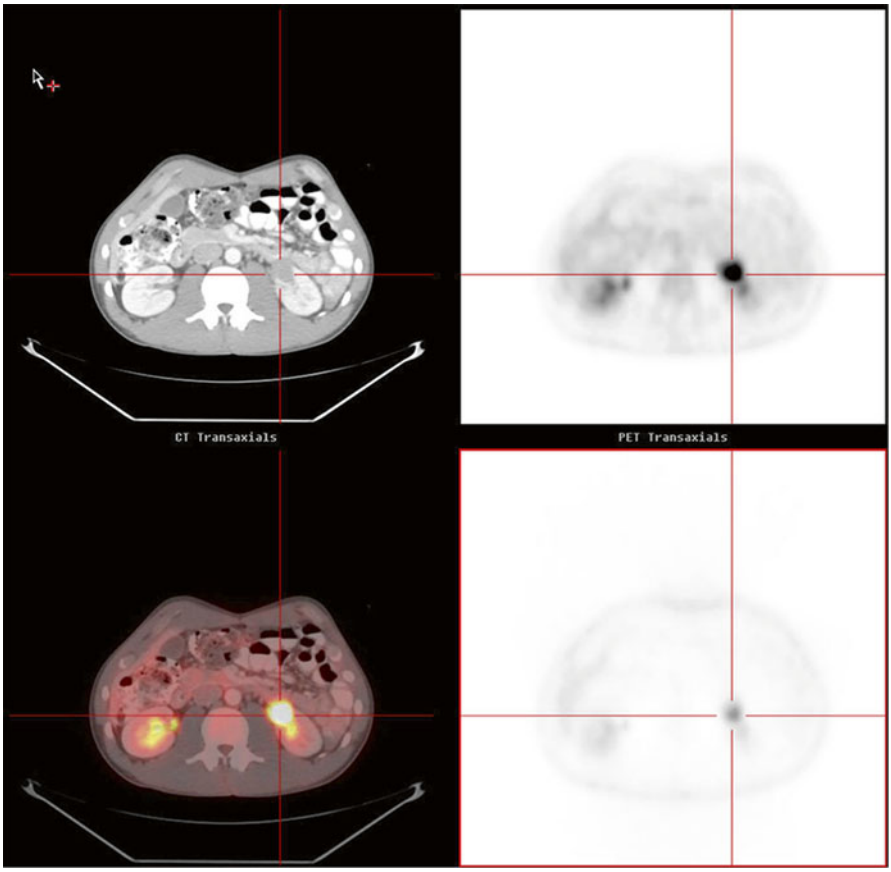

Fig. 24.2 ^{18}F-Fluorodeoxyglucose (FDG) PET/CT scan of a clear cell renal tumor located on the left kidney

only measure tumor size and have limitations in renal cancer. For example, tumors may respond to treatment and become highly necrotic; however, if the tumor size is unchanged, then RECIST fails to capture the response. Data from this study suggest that FDG-PET/CT provides a more effective means to monitor response [12].

Iodine-124-Girentuximab (cG250) PET/CT

cG250 (girentuximab, Redectane®) is a monoclonal antibody (Mab) that binds specifically to a functional epitope of CAIX. Since the transcription of CAIX is induced by HIF, it is almost universally expressed in ccRCC [13–15]. In a retrospective analysis, Choueiri et al. [16] investigated the predictive role of CAIX expression in primary tumors from patients with metastatic ccRCC. A total of 94 patients treated between August 2001 and November 2007 were included in the study. All patients

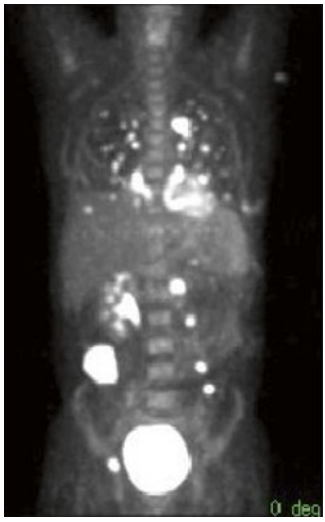

Fig. 24.3
^{18}F-Fluorodeoxyglucose (FDG) PET scan showing multiple metastatic lesions in the chest and abdomen

were treated with VEGF-targeting agents with the majority receiving sunitinib (41 %) or sorafenib (43 %). There was heterogeneity in tumor responsiveness to sunitinib or sorafenib according to CAIX status determined by immunohistochemistry. With sunitinib treatment, the average tumor shrinkage was 17 % vs. 25 % for high CAIX-expressing vs. low CAIX-expressing tumors, respectively. With sorafenib treatment, the average tumor size decreased 13 % if CAIX was high, while the average tumor size increased 9 % if CAIX was low ($p = 0.05$ for interaction). Therefore, the authors suggest that cG250 status may be a predictive biomarker for response to sorafenib treatment.

cG250 has been labeled with ^{124}I for PET imaging. cG250-PET/CT was evaluated in a phase III study that enrolled 226 presurgical patients with renal masses in 14 centers in the United States [17]. All patients had a cG250-PET/CT prior to surgery. The scans were interpreted and compared with contrast-enhanced CT by three readers who were blinded to patient information. The final tumor histology was interpreted by a single, central pathologist who was also blinded to patient information. One hundred ninety-five patients were included in the analysis. The average sensitivity was 86.2 % and 75.5 % for PET/CT and CT, respectively, for diagnosis of ccRCC. The average specificity was 85.9 % and 46.8 % for PET/CT and CT, respectively. This study concluded that the accuracy for diagnosis of ccRCC using PET/CT was comparable to biopsy. However, the results do not permit conclusions regarding other subtypes of RCC.

^{18}F-Fluoro-3′-deoxy-3′-l-fluorothymidine (FLT) PET

Shields et al. [18] first described FLT as a tracer for PET imaging. FLT is an analog of thymidine, which is normally incorporated into DNA during cellular proliferation. FLT is actively taken up by cells and monophosphorylated by thymidine kinase

1, which traps the tracer inside the cell. Intracellular FLT is resistant to degradation and directly reflects thymidine kinase 1 activity and thus cellular proliferation.

Wong et al. evaluated FLT-PET for assessing cellular proliferation in RCC. They evaluated 27 patients with newly diagnosed RCC. All patients had preoperative FLT scans. Immunohistochemical (IHC) staining using Ki-67, which correlates with cellular proliferation, was performed on all resected tumors. The degree of Ki-67 IHC staining was compared with preoperative FLT-PET imaging. FLT signal strongly correlated with Ki-67 expression [19, 20].

Lui et al. [21] used FLT-PET/CT to detect proliferative changes in RCC and other solid cancers during sunitinib treatment and withdrawal. Sixteen patients with metastatic lesions visualized on FLT-PET/CT who had no prior exposure to anti-VEGF therapy were enrolled in this study. All patients received FLT-PET/CT imaging at baseline, during sunitinib exposure, and following sunitinib withdrawal on a 4/2 or 2/1 schedule. The authors found an increase in cellular proliferation during sunitinib withdrawal in patients with RCC, which was consistent with an expected flare in angiogenesis when sunitinib is held. Interestingly, in an exploratory analysis, patients with a larger flare were less likely to benefit clinically from sunitinib therapy. Taken together, the studies of FLT-PET/CT suggest that this imaging modality may be useful in assessing tumor proliferation and directing therapy.

^{111}In-Bevacizumab (In-Bevacizumab) PET

Another promising strategy is to radiolabel active drugs for PET imaging. Bevacizumab is a humanized Mab that binds and inhibits VEGF. Bevacizumab is approved for the treatment of a variety of malignancies including RCC. Desar et al. [22] evaluated In-bevacizumab PET imaging in 14 patients with RCC who were scheduled to undergo a nephrectomy. In nine patients, neoadjuvant sorafenib was administered and In-bevacizumab PET was performed before and after sorafenib treatment. Scans were performed in five control patients who did not receive neoadjuvant therapy. In all 14 patients, In-bevacizumab preferentially accumulated in the renal tumor. After treatment with sorafenib, there was a 60.5 % reduction in the mean uptake in the primary tumor in patients with ccRCC, which correlated with decreased vascularity seen by IHC staining of the tumor. Interesting, there was no change in PET imaging or tumor vascularity in one patient with papillary RCC. This study suggests that this imaging modality may be useful for staging RCC and monitoring response to anti-angiogenic therapy.

Molecular Optical Imaging

Optical imaging is another technique for molecular imaging being applied to RCC. Optical imaging can be used noninvasively or at the time of surgery to detect molecular markers. Molecular optical imaging involves the detection of light signals emitted by various probes used to infer biologic or chemical properties of the

target tissue. Initial optical imaging research in urology was applied to the diagnosis of bladder cancer [23]. More recently, the focus has been broadened to evaluate RCC. Both fluorescence and non-fluorescence-based optical imaging techniques are being utilized.

Non-fluorescent: Tissue Spectroscopy

Optical spectroscopy (OS) is a noninvasive technique used to identify relative changes in the way light interacts with tissue. In OS, light is scattered by cell analytes or absorbed by chromophores in the tissues. Malignant cells are structurally different from normal cells, resulting in changes in optical properties. These differences are detected with spectroscopy after illumination with light [24]. OS can be used to differentiate tissue types by providing information on structure. This approach has been used to detect pancreatic tumor [25].

Parekh et al. [26] published the first ex vivo study in RCC using OS. The authors looked at kidney samples from ten patients after radical nephrectomy using OS and compared the findings to the pathology. Six patients had ccRCC, three had papillary RCC, and one had a cystic nephroma. Malignant tissue had higher reflectance intensities, ranging between 600 and 800 nm, compared to normal renal tissue.

Bensalah et al. [27] also assessed OS to reliably differentiate tumor and normal tissue in renal specimens obtained from tumors and normal parenchyma. The optical reflectance spectroscopy slopes were assessed. A total of 21 (13 radical and 8 partial nephrectomies) specimens was analyzed, and based on OS, 15 were determined to be malignant (14 ccRCC and 1 papillary), and 6 were determined to be benign (oncocytoma). There was a significant difference between the average OS spectral slopes and intensities between tumor and normal parenchyma ($p = 0.03$). The data indicate that OS may be helpful in detecting positive margins during partial nephrectomy. These studies suggest a potential role for OS in differentiating malignant and normal renal parenchyma.

Non-fluorescent: Optical Coherence Tomography (OCT)

Optical coherence tomography, first developed for ophthalmological applications, provides in situ imaging of tissue morphology with resolution approaching the micron scale (1–2 μm) with a depth of penetration of 2–4 mm. The images show the microscopic tissue structures observed in histology [28, 29].

The technique involves directing a beam of near-infrared light (1,300 nm) from a low-coherent fiber-coupled light source (e.g., a superluminescent diode) at the target tissue and detecting light that is backscattered from the targeted tissue. This phenomenon is similar to ultrasound imaging, but differs in using light rather than sound to produce cross-sectional images of tissue. The imaging depth is limited by the attenuate of light as it penetrates deeper into the tissue. The attenuation is quantified by measuring the decay of signal intensity per unit depth. The attenuation

coefficient can be derived and used to characterize tissue [30]. For example, malignant tissues have irregular nuclei resulting in a higher refractive index; the attenuation coefficient is higher compared to normal tissue.

In 2011, Barwari et al. [31] reported results from an ex vivo pilot study using OCT to differentiate malignant from normal renal tissue. The study demonstrated that the abundant cellular structures in malignant tissue resulted in a higher degree of scattering and a higher attenuation coefficient than normal renal parenchyma. A follow-up, phase I in vivo human study was performed. During surgery, OCT images were obtained from 16 renal tumors and the surrounding normal renal parenchyma. Ex vivo OCT images were also obtained. The pathology was then compared with the images. Using attenuation coefficients, there was a significant difference between normal renal parenchyma and malignant tumors. However, the difference in attenuation coefficients between malignant and benign tumors was not significant. The authors postulated that with a larger sample size, a clear difference might be found [32].

Linehan et al. [33] used OCT imaging to assess histologic subtypes of RCC. After radical or partial nephrectomy in 20 subjects, both the normal renal parenchyma and the tumor were evaluated with light microscopy and a benchtop OCT system. OCT images were compared with histological slides. OCT was most successful in distinguishing angiomyolipoma and urothelial carcinoma from normal parenchyma. OCT is less useful for identifying oncocytoma. ccRCC and other subtypes of RCC had a heterogeneous appearance, precluding reliable identification. The authors speculated that higher-resolution OCT, such as optical coherence microscopy (OCM), may be more useful for subtyping RCC.

OCM combines OCT with confocal microscopy to improve imaging depth compared to that of standard confocal microscopy [34]. Lee et al. [35] examined the use of OCT and OCM to assess human renal tissues. A total of 35 renal specimens from 19 patients, consisting of 12 normal tissues and 23 tumors (16 ccRCC, 5 papillary RCC, and 2 oncocytomas), was imaged ex vivo after surgical resection. OCT and OCM images were compared with standard histology. Three pathologists blinded to histology evaluated sensitivity and specificity of the images for differentiating normal from neoplastic renal tissues. Each imaging method was useful for assessing morphology. OCT and OCM matched well with the corresponding histology. Three observers achieved 88 %, 100 %, and 100 % sensitivity and 100 %, 88 %, and 100 % specificity, respectively, when evaluating normal vs. neoplastic specimens.

These results indicate OCT and OCM can be used to identify distinctive morphological patterns and achieve diagnostic accuracy. While the technology is limited by depth of penetration, it has the potential to serve as an adjunct during surgery since it offers the advantage of real-time pathologic information.

Fluorescence Optical Imaging

Fluorescence results when a photon is absorbed by a molecule at one wavelength and emitted at a longer wavelength. A variety of fluorescent reporters, known as fluorophores, have been described and they can be proteins, dyes, or nanoparticles.

Fluorescein is an example of a fluorophore. Fluorescein has limited use in oncology because fluorescent signals are absorbed and scattered by both normal and malignant tissues. Additionally, normal tissue produces background fluorescence in a similar wavelength spectrum as malignant cells. One strategy to overcome this limitation is to use fluorophores that emit in the near-infrared spectrum where there is minimal background fluorescence and light signals penetrate deeper into tissue. To differentiate between healthy and diseased tissue, fluorophores can be used to tag antibodies and other molecules that specifically bind disease-specific markers.

Cyanine Dyes

Indocyanine green (ICG) is a fluorescent dye that absorbs near-infrared (NIR) light and emits light at a slightly longer wavelength, which can be detected by a NIR camera. ICG binds to plasma proteins when injected intravenously. The vasculature can then be visualized with a NIR camera. Additionally, when compared to normal kidney, renal tumors have lower expression of bilitranslocase, which is the carrier protein for ICG [36]. Thus, cortical tumors are less efficient at taking up the dye and appear hypofluorescent when viewed with a NIR camera.

This technology can be applied during partial nephrectomies to achieve complete resection of the tumor. Tobis et al. reported their initial clinical experience with 11 robotic-assisted partial nephrectomies using ICG [37]. Of the malignant tumors, seven were hypofluorescent and three were isofluorescent compared to surrounding renal parenchyma. All surgical margins were negative on final pathology. They concluded that the technology aided in differentiating the tumor mass from normal parenchyma and the renal vessels.

Krane et al. [38] recently performed a prospective study using ICG in 47 consecutive patients with renal masses suspicious for malignancy who underwent robotic partial nephrectomy (RPN). This cohort was compared to 47 consecutive patients who had undergone RPN without near-infrared fluorescence. The group found no significant difference in positive margin rate or Clavien complications. There was a small decrease in warm ischemia time in the ICG group. The authors felt ICG helped identify vasculature, but it did not help with the dissection of the mass, even in cases of endophytic tumors. These early studies provide mixed results on the usefulness of intraoperative ICG, but they demonstrate a technology that has the potential to improve oncologic and functional outcomes of partial nephrectomy.

Fluorescence: 5-Aminolevulinic Acid (5-ALA)

5-ALA is metabolized to protoporphyrin IX, a fluorescent agent. Protoporphyrin IX accumulates in rapidly proliferating cells, thus allowing differentiation of malignant versus normal parenchyma [39]. 5-ALA was first studied in a murine model and showed promise for identification of malignant tumors [40]. Hoda et al. [41] applied this technology to RCC in a prospective, non-randomized single-center study.

The authors described the use of protoporphyrin IX imaging for detection of malignant renal masses and to evaluate surgical margin status during laparoscopic partial nephrectomy. This imaging modality had a sensitivity of 95 % and specificity of 94 % in identification of a renal tumor as RCC. Furthermore, they reported a sensitivity of 100 % for detection of positive margins.

Conclusions

PET and optical imaging techniques are being actively evaluated in the management of RCC. PET has the potential to provide noninvasive means of determining histology and malignant potential of a renal mass. Patients with localized disease can be risk-stratified for observation, nephron-sparing surgery, or radical nephrectomy. Patients with metastatic disease may be imaged to determine the best therapy, and treatment response can be monitored with serial imaging.

Preliminary studies in optical imaging offer promise in differentiation of normal from malignant renal tissue. Optical imaging techniques have potential to provide histological information without the need to remove the tissue from the patient. This information may be used to diagnose RCC or used intraoperatively to assess surgical margins during partial nephrectomy.

Many of these techniques remain investigational and validation of early results is necessary, but the potential advantages are clear. Further advances in our understanding of the molecular basis of RCC are expected to produce parallel advances in strategies for molecularly targeted imaging.

References

1. Siegel R, Ahmedin J. Cancer statistics, 2013. CA Cancer J Clin. 2013;63:11–30.
2. Levy DA, Dinney CP. Stage specific guidelines for surveillance after radical nephrectomy for local renal cell carcinoma. J Urol. 1998;159:1163–7.
3. Pantuck AJ, Belldegrun AS. The changing natural history of renal cell carcinoma. J Urol. 2001;166:1611–23.
4. Figlin RA. Renal cell carcinoma: management of advanced disease. J Urol. 1999;161:381–6. discussion 6–7.
5. Gnarra JR, Tory K, Weng Y, et al. Mutations of VHL tumour suppressor gene in renal carcinoma. Nat Genet. 1994;7(1):85–90.
6. Cowey CL, Rathmell WK. Using molecular biology to develop drugs for renal cell carcinoma. Expert Opin Drug Discov. 2008;3:311–27.
7. Cowey CL, Rathmell WK. VHL gene mutations in renal cell carcinoma: role as a biomarker of disease. Curr Oncol Rep. 2009;11(2):94–101.
8. Kang DE, Teigland CM. Clinical use of fluorodeoxyglucose F 18 positron emission tomography for detection of renal cell carcinoma. J Urol. 2004;171(5):1806–9.
9. Nakatani K, Togashi K. The potential clinical value of FDG-PET for recurrent renal cell carcinoma. Eur J Radiol. 2011;79(1):29–35.

10. Wang HY, Ding HJ, Chen JH, et al. Meta-analysis of the diagnostic performance of [18]FDG-PET and PET/CT in renal cell carcinoma. Cancer Imaging. 2012;12:464–74.
11. Kayani I, Avril N, Bomanji J, et al. Sequential FDG-PET/CT as a biomarker of response to Sunitinib in metastatic clear cell renal cancer. Clin Cancer Res. 2011;17(18):6021–8.
12. Papazisis KT, Kontovinis LF, Papandreou, et al. Sunitinib treatment for patients with clear cell metastatic renal cell carcinoma: clinical outcomes and plasma angiogenesis markers. BMC Cancer. 2009;9:82.
13. Lam JS, Figlin RA. G250: a carbonic anhydrase IX monoclonal antibody. Curr Oncol Rep. 2005;7(2):109–15.
14. Oosterwijk E, Debruyne FM. Radiolabeled monoclonal antibody G250 in renal-cell carcinoma. World J Urol. 1995;13(3):186–90.
15. Grabmaier K, Vissers JL, De Weijert MC, et al. Molecular cloning and immunogenicity of renal cell carcinoma-associated antigen G250. Int J Cancer. 2000;85(6):865–70.
16. Choueiri TK, Regan MM, Rosenberg JE, et al. Carbonic anhydrase IX and pathological features as predictors of outcome in patients with metastatic clear-cell renal cell carcinoma receiving vascular endothelial growth factor-targeted therapy. BJU Int. 2010;106:772–8.
17. Divgi CR, Uzzo RG, Gatsonis C, et al. Positron emission tomography/computed tomography identification of clear cell renal cell carcinoma: results from the REDECT trial. J Clin Oncol. 2013;31(2):187–94.
18. Shields FA, Greirson JR, Dohmen BM, et al. Imaging proliferation in vivo with [F-18]FLT and positron emission tomography. Nat Med. 1998;4(11):1334–6.
19. Wong P, Bolton DM, Lee ST, et al. In-vivo imaging of cellular proliferation in renal cell carcinoma using [18]F-FLT PET. J Urol. 2009;181(4):155.
20. Vesselle H, Grierson J, Muzi M, et al. In vivo validation of 3′ deoxy-3′-[(18)F]fluorothymidine ([(18)F]FLT) as a proliferation imaging tracer in humans: correlation of [(18)F]FLT uptake by positron emission tomography with Ki-67 immunohistochemistry and flow cytometry in human lung tumors. Clin Cancer Res. 2002;8:3315–23.
21. Liu G, Jeraj R, Vanderhoek M, et al. Pharmacodynamic study using FLT PET/CT in patients with renal cell cancer and other solid malignancies treated with sunitinib malate. Clin Cancer Res. 2011;17(24):7634–44.
22. Desar IM, Stillebroer AB, Oosterwijk E, et al. 111In-bevacizumab imaging of renal cell cancer and evaluation of neoadjuvant treatment with the vascular endothelial growth factor receptor inhibitor sorafenib. J Nucl Med. 2010;51:1707–15.
23. Cauberg EC, deBruin DM, Faber DJ, et al. A new generation of optical diagnostics for bladder cancer: technology, diagnostic accuracy, and future applications. Eur Urol. 2009;56:287–9.
24. Amelink A, Sterenborg HJ, Bard MP, et al. *In vivo* measurements of the local optical properties of tissue by use of differential path-length spectroscopy. Opt Lett. 2004;29:1087–96.
25. Brand Y, Liu R, Turzhitsky V, et al. Optical markers in duodenal mucosa predict the presence of pancreatic cancer. Clin Cancer Res. 2007;13:4392–9.
26. Parekh DJ, Herrell SD. Optical spectroscopy characteristics can differentiate benign and malignant renal tissues: a potentially useful modality. J Urol. 2005;174:1754–8.
27. Bensalah K, Tuncel A, Peshwani D, et al. Optical reflectance spectroscopy to differentiate renal tumor from normal parenchyma. J Urol. 2008;179:2010–3.
28. Huang D, Swanson EA, Lin CP, et al. Optical coherence tomography. Science. 1991;254:1178–81.
29. Crow P, Stone N, Kendall CA, et al. Optical diagnostics in urology: current applications and future prospects. BJU Int. 2003;92:400–7.
30. Faber D, van der Meer F, Aalders M, et al. Quantitative measurement of attenuation coefficients of weakly scattering media using optical coherence tomography. Opt Express. 2004;12:4353–65.
31. Barwari K, de Bruin DM, Cauberg EC, et al. Advanced diagnostics in renal mass using optical coherence tomography: a preliminary report. J Endourol. 2011;25:311–5.
32. Barwari K, de Bruin DM, Faber DJ, et al. Differentiation between normal renal tissue and renal tumours using functional optical coherence tomography: a phase I in vivo human study. BJU Int. 2012;110(8 PT B):E415–20. doi:10.1111/j.1464-410X.2012.11197.x. Epub 2012 May 10.

33. Linehan JA, Bracamonte ER, Hariri LP, et al. Feasibility of optical coherence tomography imaging to characterize renal neoplasms: limitations in resolution and depth of penetration. BJU Int. 2011;108(11):1820–4.
34. Izatt JA, Hee MR, Owen GM, et al. Optical coherence microscopy in scattering media. Opt Lett. 1994;19:590.
35. Lee HC, Zhou C, Cohen DW, et al. Integrated optical coherence tomography and optical coherence microscopy imaging of ex vivo human renal tissues. J Urol. 2012;187(2):691–9. doi:10.1016/j.juro.2011.09.149. Epub 2011 Dec 16.
36. Golijanin DJ, Marshall J, Cardin A, et al. Bilitranslocase(BTL) is immunolocalised in proximal and distal renal tubules and absent in renal cortical tumors accurately corresponding to intraoperative near infrared fluorescence (NIRF) expression of renal cortical tumors using intravenous indocyanine green (ICG). J Urol. 2008;179(4):137. abstract 386.
37. Tobis S, Knopf J, Silvers C, et al. Near infrared fluorescence imaging with robotic assisted laparoscopic partial nephrectomy: initial clinical experience for renal cortical tumors. J Urol. 2011;186:47–52.
38. Krane LS, Hemal AK. Is near infrared fluorescence imaging using indocyanine green dye useful in robotic partial nephrectomy: a prospective comparative study of 94 patients. Urology. 2012;80:110–8.
39. Peng Q, Warloe T, Berg K, et al. 5-aminolevulinic acid-based photodynamic therapy. Clinical research and future challenges. Cancer. 1997;79(12):2282–308.
40. Popken G, Schultze-Seemann W. Kidney-preserving tumour resection in renal cell carcinoma with photodynamic detection by 5-aminolaevulinic acid: preclinical and preliminary clinical results. BJU Int. 1999;83:578–82.
41. Hoda MR, Popken G. Surgical outcomes of fluorescence-guided laparoscopic partial nephrectomy using 5-aminolevulinic acid-induced protoporphyrin IX. J Surg Res. 2009;154:220–5.